

# $\tau - \rho$ Algorithm in the Application of Rayleigh Wave Monitoring

Jun Qiao<sup>1</sup>, Naying Li<sup>2</sup>, Fangyong Li<sup>3</sup>, Tianhan Li<sup>1</sup>

<sup>1</sup>School of Civil Engineering & Architecture, Chongqing Jiaotong University, Chongqing, 400074, CHINA

<sup>2</sup>School of Civil Engineering English, Chongqing Jiaotong University, Chongqing, 400074, CHINA

<sup>3</sup>School of Enterprise Management, Chongqing Jiaotong University, Chongqing, 400074, CHINA

**Abstract:** Rayleigh wave exploration has advantages of high efficiency, low cost and easy practice, and it is applied broadly in engineering. This article, combined with highway detection, study how to make use of conversion to abstract Rayleigh wave, and according to the Rayleigh wave data, it can invert out the sub grade compaction. From the comparison between sub grade compaction and core compaction, it is noted that  $\tau - \rho$  conversion was good to solve the problem of Rayleigh wave separation, and  $\tau - \rho$  conversion can advance the detection precision and longitudinal and lateral resolution of Transient Rayleigh Wave Method.

**Keywords:** Rayleigh wave;  $\tau$ - $\rho$  conversion; Sub grade compaction

## 1. Introduction

Rayleigh wave exploration has advantages of high efficiency low cost and easy practice, and it is applied broadly in engineering. The main idea of Rayleigh wave exploration is to make use of its frequency dispersion to reflect the problems of low layer. And Rayleigh wave exploration is divided into steady state way and transient state way according to the differ of explode mode. Nowadays, there are a lot of modes to abstract Rayleigh wave, while we adopt  $\tau$ - $\rho$  modes.  $\tau$ - $\rho$  mode use  $\tau$ - $\rho$  conversion (slant stack) to abstract Rayleigh wave and the Rayleigh wave record meets the requirement of using adjacent-channel to calculate the dispersion curves. This resolves the multi-channel comprehensive effect, which cannot test the small-scale and local anomaly.  $\tau$ - $\rho$  conversion improves the detecting precision and the longitudinal and vertical resolution of TRWM. (Transient Rayleigh Wave Method).

## 2. The Ultimate Principle of $\tau$ - $\rho$ Conversion

$\tau$ -  $\rho$  conversion is a kind of discredited conversion , and it's ultimate principle is that the seismic records of one common shot gather , which is in the time-space domain (x-t domain), can be mapped to  $\tau$ -  $\rho$  domain under the mode of  $\tau$ -  $\rho$  forward transform us follows ,

$$\Psi(p, t) = \sum \Phi(x, t + px) \quad (1)$$

$$t = t - px \quad (2)$$

$$p = dt / dx = 1 / v^* = \sin \theta / v \quad (3)$$

In those formulas, the physical significance of parameterize vertical wave slowness; the geometrical significance of it is the intercept on the timer shaft in  $\tau$ - $\rho$  conversion .The physical significance of  $\rho$  is that the longitu-

dinal wave slowness is the reciprocal of the longitudinal apparent velocity, and it is related to the incident angle .On the aspect of geometric  $\rho$  is the rag parameter (or the transient slop of time curve).  $v^*$  is apparent velocity,  $\theta$  is the incident angle of traveling wave ray;  $v$  is the medium-speed.

After transition, the cross interference complex wave fields were separated individually in the domain. In the domain of  $\tau$ - $\rho$ , the reflection hyperbolic curve lineups were mapped to an ellipse in the domain; the surface wave, direct wave, sound wave and refracted wave, with characteristic of linear event, were transformed to the separate individual points under the condition, where  $\tau$ - $\rho$  is a constant value. Then, it can separate the wave fields and extracts seismic signals which are needed. Inverse transformation varies from  $\tau$ -  $\rho$  space to the original x-t space, the formula is:

$$\Phi(x, t) = \sum \Psi(p, t - px) \quad (4)$$

The formulas, which are shown in (1) and (4), can transform to discrete version, and they respectively are:

$$\Psi(P_j, t_j) = \sum_{n=1}^N \Phi(x_n, t_j + P_j x_n) \quad (5)$$

$$\Phi(x_n, t_m) = \sum_{j=1}^J \Psi(P_j, t_m - P_j x_n) \quad (6)$$

$$u_1(t) = A_2 \cos w(t - \frac{x_1}{V_R}) \quad (7)$$

And,  $i=1,2, \dots, I$ ;  $j=1,2,\dots,J$ ;  $n=1, 2, \dots, N$ ;  $m= 1, 2, \dots, M$ ;  $N$  is the channel number of multi-channel gathers seismic records;  $M$  is the sampling points of each record ;  $I$  is the number of channel  $\rho$  .

### 2.1. Process flows and the function of each flow

The original records are the swing values of Rayleigh waves, direct wave, reflection wave, sound wave and random disturbance, which is varied with time changing, and these waves was impacted by earth filtering and spherical spreading. So, to obtain the final compaction as the nondestructive testing sugared quality's explanation result, it needs a series of dealing such as true aptitude recovery, spectral analysis, smoothing and Rayleigh wave abstraction, adjacent-channel dispersion curve's calculation, transversal wave velocity inversion and compaction obtaining.

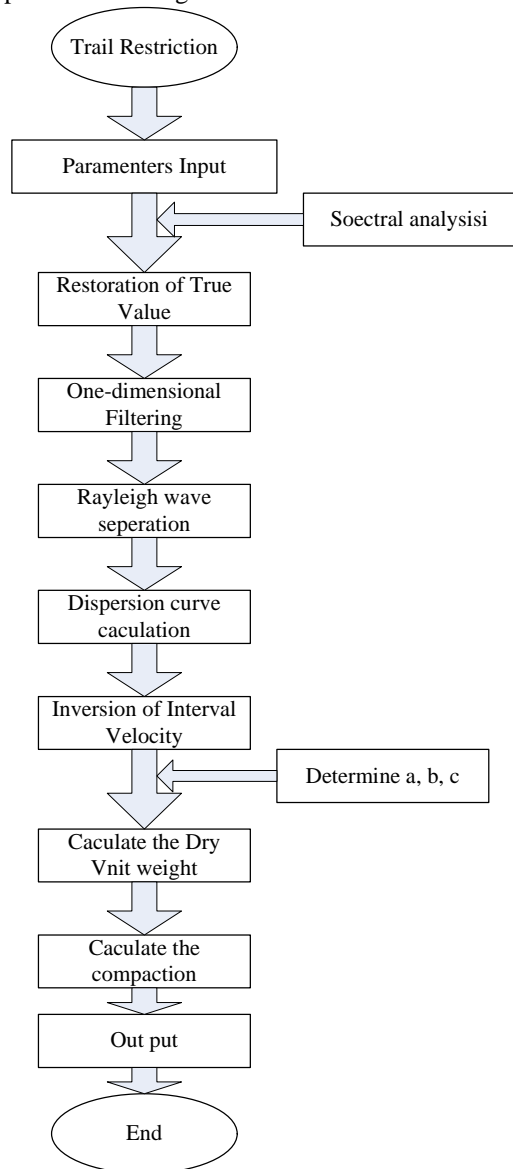


Figure 1. Treatment Scheme

With a lot of selection and comparison of parameter and treatment scheme, the main treatment scheme was determined as Fig 1, and the function of each process is shown in below .

- (1) Restoration of true swing value: to eliminate the effect by the earth filtering and spherical spread.
- (2) Spectral Analysis: to obtain effective wave frequency band.
- (3) One-dimensional filtering: to eliminate the interference of LF (low-frequency) and HF (high-frequency).
- (4) Separating Rayleigh wave by  $\tau$ -  $\rho$  conversion: to eliminate the disturbance of direct wave, reflect wave, sound wave and random disturbance and to obtain Rayleigh wave.
- (5) Calculating adjacent-channel dispersion curve: frequency dispersion curve, also is the related curve with average velocity and frequency or the 1/2 wavelength of Rayleigh wave.
- (6) Inversion of interval velocity : to use dispersion curve with the damped least square method and back calculate out the thickness and corresponding S-wave interval velocity of each layer.
- (7) Calculate a, b, c and the compaction: based on the compaction of every fixed point layer, and use the least square method to make inversion fitting analysis. And then, to obtain compaction lateral wave speed, and the undetermined coefficient a, b and c (in formula (7)). Finally, to calculate out the compaction by use of (7).
- (8) Output: to output the result data and map figure.

### 3. Result and Interpretation of Result

#### 3.1. $\tau$ - $\rho$ conversion technique and rayleigh wave record

(1) The Abstraction Experiment of Rayleigh wave. In Fig 2, there is an original record of a common –source point in the test section. According the record , it is noted that Rayleigh wave can be distinguished easily , and compared with other waves , it has strongest amplitude . But it is still disturbed by direct wave, reflect wave and random disturbance, and all of the waves were mutual disturbed too.

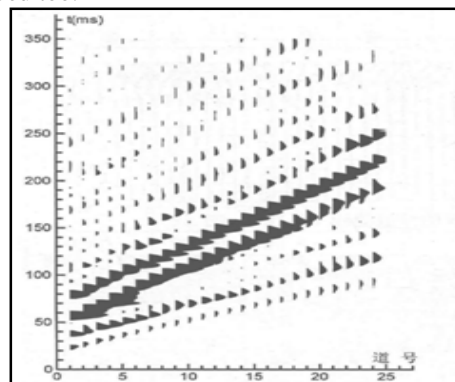


Figure 2. The Original Record of Common-source points

After  $\tau$ - $\rho$  conversion, Rayleigh wave, with stronger strength, can be distinguished easily, and it mainly concentrates in an ovals hap area. The energies of other

waves are relatively weak and rather dispersed. These features conform to the theoretical records. After eliminating the disturbance of the direct wave, reflect wave and interference wave,  $\tau$ - $\rho$  inverse transformation Rayleigh wave records are shown in Fig 2. From this Fig, it is noted that the disturbance of direct wave and reflect wave had been abstracted correctly.

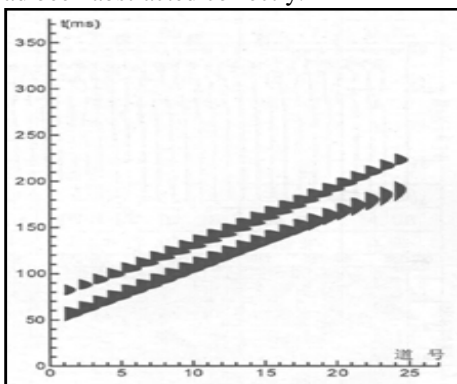


Figure 3. The Rayleigh Wave Record of Common-source Point

(2) The Rayleigh Records of Test section

Fig 4 is the common-source point records, which had been separated by  $\tau$ - $\rho$  conversion. From this Fig, it is obvious that the disturbance had been eliminated and Rayleigh waves were effectively separated with a clear dispersion character.

3.2. Adjacent-channel dispersion curve

Fig 5 and Fig 6 is adjacent-channel dispersion curve. From the Figures, it is obvious that the dispersion curves have smooth curve clear inflection point, good longitudinal regularity, and obvious local anomaly. It meets the requirement of inversion. It shows that the Rayleigh wave which is abstracted with  $\tau$ - $\rho$  conversion method can adopt in the calculation of adjacent-channel frequency dispersion curve, and this can advance the vertical and horizontal resolution ratio of non-destructive Rayleigh wave test.

3.3. Coefficients a, b and c

Select ck0+195 and ck0+225 as the fixed points, the values can be found in the Table 1. Put the value of Table 1 in the mode (2-60) and (2-61), it can be determined that  $a = 0.2711$ ,  $b = -0.0047$ ,  $c = 0.3200$ .

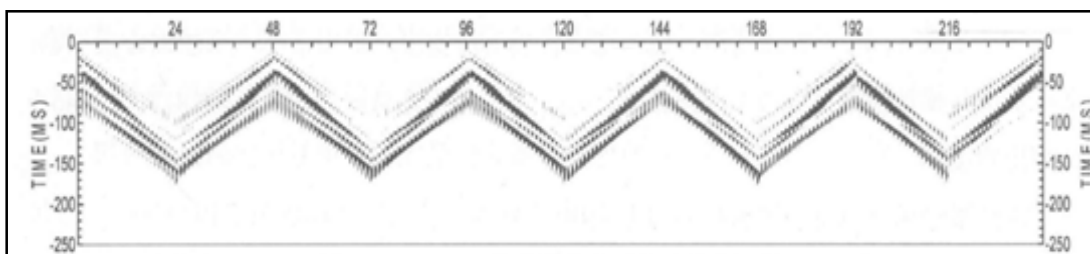


Figure 4. The Common-source Point Records after  $\tau$ - $\rho$  Conversion and Separation

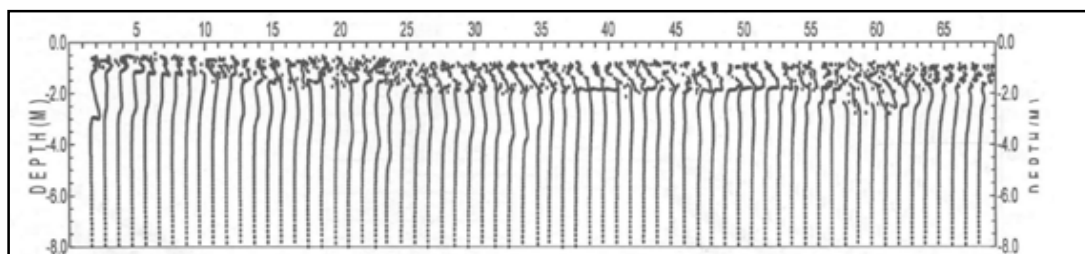


Figure 5. The Dispersion Curve by  $\tau$ - $\rho$  conversion Mode

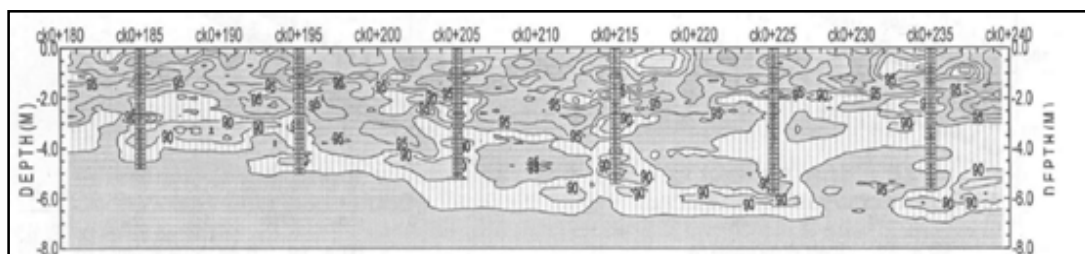


Figure 6. The compaction distribution diagram by  $\tau$ - $\rho$  Conversion Mode

**Table 1. The Comparative Statement of  $\tau$ -  $\rho$  Conversion Results**

	CK0+185			CK0+195			CK0+205		
	Core com- paction	Measured compaction	Error	Core com- paction	Measured compaction	Error	Core com- paction	Measured compaction	Error
	(%)	(%)	(%)	(%)	(%)	(%)	(%)	(%)	(%)
0.20	94.90	95.46	0.56	95.40	95.55	0.15	96.60	96.70	0.1
0.40	98.90	97.78	1.12	96.60	96.51	0.09	97.10	96.73	0.37
0.60	95.90	96.97	1.07	97.10	97.37	0.27	95.30	94.82	0.48
0.80	94.20	95.44	1.24	93.60	95.37	1.77	90.70	91.90	1.2
1.00	94.80	93.99	0.81	92.40	94.88	2.48	89.50	93.20	3.7
1.20	100.06	97.08	2.98	105.20	101.80	3.4	105.20	101.30	3.9
1.40	102.30	99.08	3.22	101.20	101.10	0.1	98.30	98.94	0.64
1.60	94.20	95.84	1.64	100.00	98.13	1.87	94.20	96.47	2.27
1.80	94.80	94.45	0.35	93.10	93.69	0.59	93.60	94.52	0.92
2.00	89.70	91.50	1.80	89.10	91.30	2.2	93.70	92.85	0.85
2.20	91.40	91.35	0.05	90.20	91.97	1.77	90.20	90.77	0.57
2.40	89.70	91.32	1.62	93.70	93.25	0.45	93.10	90.85	2.25
2.60	92.50	94.85	2.35	89.10	91.70	2.6	80.50	86.30	5.8
2.80	110.90	102.44	8.46	91.40	91.42	0.02	85.60	87.88	2.28
3.00	89.70	92.44	2.74	94.30	92.14	2.16	92.00	91.86	0.14
3.20	91.40	90.78	0.62	86.30	88.79	2.49	90.90	91.96	1.06
3.40	88.00	89.25	1.25	91.40	90.88	0.52	91.40	91.24	0.16
3.60	86.20	87.90	1.70	87.90	90.00	2.1	89.70	89.64	0.06
3.80	85.60	87.73	2.13	87.90	89.75	1.85	82.20	86.29	4.09
4.00	90.80	90.58	0.22	87.40	90.91	3.51	90.80	90.30	0.5
4.20	89.80	90.36	0.56	93.70	93.44	0.26	92.60	91.60	1
4.40	86.90	89.80	2.90	88.00	89.96	1.96	86.30	88.41	2.11
4.60	94.40	93.36	1.04	89.70	90.07	0.37	85.20	87.44	2.24
4.80	93.60	93.78	0.18	90.02	91.12	1.1	90.20	89.98	0.22
5.00							90.80	90.41	0.39
5.20							89.60	90.21	0.61
Minimum Value	85.60	87.73	0.05	86.30	88.79	0.02	80.50	86.29	0.06
Maximum Value	110.90	102.44	8.46	105.20	101.80	3.51	105.20	101.30	5.8
Average	93.38	93.48	1.69	92.78	93.37	1.42	91.36	92.02	1.46

**3.4. The interpretation and analysis of compaction result**

From Fig 4, it is noted that the bottom margin of road base backfill is distinct. The compaction of the junction between road base backfill and original road base is lower. Core compaction in various layers, compared with the fixed point's ck0+195 and ck0+225, the maximal relative error is 9.62%, and the minimal one is 0.02%, the average one is 1.60%. There are 14 points whose relative error is larger than 3.5%. These 14 points is 8.48% of all, and they are all at the abrupt change point of compaction.

The main reason that cause these error is that core testing results represent a synthesis result of a papilla , while the transient Rayleigh wave mode represents the synthesis result of the adjacent-channel (In this test , there is 1m between every two channel . ) . So, there must be error between the two, and the error is related to the uniformity of the medium and the trace spacing. The higher uniformity and smaller trace spacing will provide the smaller errors, so, it is noted that one can improve the direction precision by means of reducing the trace spacing. The results and comparative analysis are shown in Table 2.

**Table 2.  $\tau$ -  $\rho$  Transform results and the comparative analysis**

	CK0+215			CK0+225			CK0+235		
	Core com- paction	Measured compaction	Error	Core com- paction	Measured compaction	Error	Core com- paction	Measured compaction	Error
	(%)	(%)	(%)	(%)	(%)	(%)	(%)	(%)	(%)
0.20	99.40	97.87	1.53	101.10	100.42	0.68	98.20	97.48	0.72
0.40	89.10	91.59	2.49	95.90	96.43	0.53	92.50	93.34	0.84
0.60	94.20	93.08	1.12	94.20	95.10	0.90	91.90	91.46	0.44
0.80	93.10	95.74	2.64	98.30	98.20	0.10	89.00	90.82	1.82
1.00	102.90	100.44	2.46	101.70	100.81	0.89	100.00	96.78	3.22
1.20	104.90	101.21	3.69	99.40	99.89	0.49	94.30	95.07	0.77
1.40	97.10	98.24	1.14	99.40	98.05	1.35	100.00	96.49	3.51
1.60	99.40	95.18	4.22	91.40	95.04	3.64	94.90	94.40	0.50
1.80	76.40	83.90	7.50	106.30	100.96	5.34	91.40	92.23	0.83
2.00	91.40	89.56	1.84	91.40	93.55	2.15	91.40	91.52	0.12
2.20	95.40	92.53	2.87	93.10	91.98	1.12	89.00	90.78	1.78
2.40	89.60	91.23	1.63	89.00	90.70	1.70	88.40	90.00	1.60
2.60	93.60	92.73	0.87	90.20	90.98	0.78	91.30	91.11	0.19
2.80	87.90	89.05	1.15	89.00	90.86	1.86	90.80	91.41	0.61
3.00	85.10	87.18	2.08	89.10	90.10	1.00	91.40	91.76	0.36
3.20	86.90	88.29	1.39	89.70	89.72	0.02	93.70	92.13	1.57
3.40	89.70	90.55	0.85	89.10	89.78	0.68	89.70	90.83	1.13
3.60	93.70	93.00	0.70	90.80	90.73	0.07	94.80	93.00	1.80
3.80	90.20	91.17	0.97	92.50	91.52	0.98	90.20	91.65	1.45
4.00	87.40	89.22	1.82	89.10	90.68	1.58	93.70	93.29	0.41
4.20	89.40	89.41	0.01	94.10	92.76	1.34	95.70	94.58	1.12
4.40	83.70	87.30	3.60	91.20	91.67	0.47	92.90	93.11	0.21
4.60	91.70	90.16	1.54	91.70	91.68	0.02	91.70	91.64	0.06
4.80	84.80	86.80	2.00	89.50	90.36	0.86	88.30	90.34	2.04
5.00	82.30	85.25	2.95	87.20	88.96	1.76	94.10	93.45	0.65
5.20	90.60	89.72	0.88	87.20	89.71	2.51	94.70	94.39	0.31
5.40	91.30	91.34	0.04	97.70	95.51	2.19	93.60	93.97	0.37
5.60				95.40	95.66		94.80	93.86	
5.80				96.00	95.32				
Minimum Value	76.40	83.90	0.01	87.20	88.96	0.02	88.30	90.00	0.06
Maximum Value	104.90	101.21	7.50	106.30	100.96	5.34	100.00	97.48	3.51
Average	91.16	91.55	2.00	93.47	93.69	1.30	92.94	92.89	1.05

**4. Conclusion**

Combined with the real highway test and made use of the test of  $\tau$ -  $\rho$  conversion mode, the  $\tau$ -  $\rho$  conversion had solved the segregation of Rayleigh Wave. The Rayleigh wave records fully meet the requirement of dispersion curve which calculating by the way of adjacent-channel. From all these, it is obvious that  $\tau$ - $\rho$  conversion can high-

ly improve the detecting precision and vertical and horizontal resolution of the transient Rayleigh Wave.

**References**

[1] Tat ham R H, Goose D V. Separation of S-wave and p-wave reflections offshore western Florida [J], Geophysics, 1984, 49 (5): 493-508.

- 
- [2] Pollitz F F, Hennem C G. Analysis of Rayleigh wave refraction from three-component seismic spectra [J]. *Geophys. J. Int.*, 1993, 78 (113): 629-650.
- [3] Prabhu Rajopal, Krishnan Balasubramaniam, A new approach to inversion of surface wave dispersion relation for determination of depth distribution of non-uniform stresses in elastic materials, *International Journal of Solids and Structures*, 42(2005), P789-803
- [4] V.M.Babieh, N.h.Kirpiehnikova. A new approach to the problem of the Raleigh wave propagation along the boundary of a non-homogeneous elastic body, *Wave Motion*, 40(2004), P209-223
- [5] [5] Daniel Nkemzi, A new formula for the velocity of Raleigh waves, *wave Motion*, 26(1997), P199-205
- [6] Daniel Royer, A study of the eular equation for Rayleigh waves using the root locus method, *Ultrasonics*, 39(2001), P223-225
- [7] Michael J. Vellekoop, Acoustic wave sensors and their technology, *Ultrasonics*, 36(1998), p7-14
- [8] T.-T. Wtlu-L.Liu, Advancement on the non-destructive evaluation of concrete using transient elastic Waves, *Ultrasonics*, 36(1998), P19-204
- [9] panayotis, Amplitude equations for non-linear leigh waves, *physics Letters A*, 289(2001), P111-120
- [10] GB 50218-94, standards of engineering rock mass [S]. Beijing: China Planning Press, 1995.
- [11] ABAQUS Inc. Abacus theory manual and user's manual version 6.10[K]. Providence, RI: ABAQUS Inc.
- [12] Batley P, Gjelsvik A. Coefficient of friction for steel on concrete at high normal stress [J]. *Journal of Materials in Civil Engineering*, 1990, 2(1): 46-49.
- [13] KHAN A. Numerical modelling of shear socketed piers [J]. *International Journal for Numerical and Analytical Methods in Aeromechanics*, 2000, 24(11): 853-867